Transfer Learning-Based Osteoporosis Classification Using Simple Radiographs

https://doi.org/10.3991/ijoe.v19i08.39235

Pooja S Dodamani(✉), Ajit Danti
Christ University, Bangalore, Karnataka, India
pooja.dodamani@res.christuniversity.in

Abstract—Osteoporosis is a condition that affects the entire skeletal system, resulting in a decreased density of bone mass and the weakening of bone tissue's micro-architecture. This leads to weaker bones that are more susceptible to fractures. Detecting and measuring bone mineral density has always been a critical area of focus for researchers in the diagnosis of bone diseases such as osteoporosis. However, existing algorithms used for osteoporosis diagnosis encounter challenges in obtaining accurate results due to X-ray image noise and variations in bone shapes, especially in low-contrast conditions. Therefore, the development of efficient algorithms that can mitigate these challenges and improve the accuracy of osteoporosis diagnosis is essential. In this research paper, a comparative analysis was conducted Assessing the accuracy and efficiency of the latest deep learning CNN model, such as VGG16, VGG19, DenseNet121, Resnet50, and InceptionV3 in detecting to Classify Normal and Osteoporosis cases. The study employed 830 X-ray images of the Spine, Hand, Leg, Knee, and Hip, comprising Normal (420) and Osteoporosis (410) cases. Various performance metrics were utilized to evaluate each model. The findings indicate that DenseNet121 exhibited superior performance with an accuracy rate of 93.4% Achieving an error rate of 0.07 and a validation loss of only 0.57 compared with other models considered in this study.

Keywords—DXA, CNN models, BMD, X-rays

1 Introduction

Osteoporosis disease is a prevalent condition, particularly among postmenopausal women, and is often only diagnosed after a fracture occurs. [17] Early detection is crucial to prevent fractures occurring from Osteoporosis, which is more common in India than stroke, breast cancer, and heart attack combined. If there is an imbalance in Bone formation compared to Reabsorption then disease occurs. [46] In high-income countries, osteoporotic fractures also result in more hospital admissions than these other diseases, according to a WHO report. Hip fractures, in particular, can lead to ambulation limitations, Loss of self-sufficiency, chronic pain, and reduced quality of life and disability. [24]

DXA is considered the most accurate method for diagnosing osteoporosis and is widely accepted as the gold standard, but it is not a viable screening tool in many developing countries due to its limited availability and high cost. Therefore, researchers are continuously working to create a tool for screening osteoporosis using simpler radiographic data. [5]

There are several imaging methods available for diagnosing osteoporosis, each with its benefits and drawbacks. [27] Presently, DXA is the most commonly employed technique in clinical settings. The World Health Organization (WHO) created the Fracture Risk Assessment Tool (FRAX®) which can complement DXA, enhancing its clinical usefulness and the cost-effectiveness of treatments. Radiographic features that suggest osteoporosis, as well as Vertebral fractures, which are reliable indicators of upcoming fractures, have the potential to be predicted and are reported more effectively to increase appropriate referrals for DXA testing. Quantitative CT provides advantages over DXA, such as the ability to measure Volumetric density can be evaluated by separately measuring cortical and trabecular bone density, as well as by assessing bone shape and size, but remains mainly a research tool. High-resolution imaging, including CT and MRI, can measure cortical bone microstructure and trabecular structure, but these methods are technically demanding and not widely available for clinical use. Ensemble models are also used in Deep learning for the classification of Severe diseases. [47]

Research in the recent past has focused on exploring the use of artificial intelligence (AI) for medical image interpretation, which includes the creation of a tool to screen for osteoporosis. While some trials have used machine learning or deep learning algorithms based on radiographic data to predict osteoporosis, some of the challenges include issues like unsuitable object detection and small sample sizes, as well as methodological flaws that have hindered the creation of a reliable tool. [15]

To address these limitations, this study aims to predict osteoporosis using pre-trained models and transfer learning-based Fastai library, pre-trained models. [34] The deep learning model developed in our research represents a potential tool for osteoporosis screening, utilizing the new advancements in Medical Sector. Exceptional performance has been demonstrated by Convolutional Neural Networks (CNNs) in medical image classification, with models like VGG16, VGG19, DenseNet121, InceptionV3, and Resnet50 [22, 26, 39] being among the most effective. However, due to the limited data availability of annotated medical images, training CNNs from scratch is often impractical. To overcome this challenge, researchers have proposed the use of transfer learning, where a pre-trained CNN model trained on a large dataset can be fine-tuned using the small dataset for the latest problem. Employing the understanding obtained from the vast dataset, transfer learning enables the CNN model to quickly adapt to the new dataset and effectively classify the images. [4]

2 Literature review

Zhang et al. [44] proposed a method of classifying bone mineral density (BMD) in postmenopausal women using routine lumbar spine X-ray images. This innovative approach can help Individuals who are at risk of developing osteopenia and osteoporosis,

that need more Enhanced screening while reducing radiation exposure or significant costs accessibility. It should be noted that while this deep learning model cannot completely replace the traditional method Dual-energy X-ray absorptiometry (DXA) to access BMD, can be a useful alternative in situations where lumbar spine X-rays are available and DXA is not been performed yet. Before prospectively conducting clinical trials, it may be necessary to access the efficacy of the suggested model in predicting fracture risk using retrospective data. The DCNN model has channels for performing analysis of lateral and anterior-posterior lunar spine images. Each channel has the input of 64 x 64 patches region of interest to extract the potential features of texture and Edge related features to improve the performance within the receptive field. The captured patches were sent to the model to filter less and highly relevant features later it was classified as normal, osteopenia, and osteoporosis. Limitations in the study The calculations and the potential features used by the model are difficult to predict. Also, DXA has a fixed positioning when it comes to the measurement of bone mass density which can lead to overestimation due to the overlying structure of the spine. The study focused on osteoporosis classification of women who are aged only above 50 years further investigations of less age need to be done.

Yassine Nasser et al. [23] proposed a method that leverages the effectiveness of deep learning techniques to get important information using X-ray images to distinguish between osteoporosis and healthy subjects. However, there are two main challenges in diagnosing osteoporosis using this approach: the difficulty in visually distinguishing between the two conditions and the need for a large dataset to train deep learning networks. To address these challenges, our method involves three steps: 1) pre-processing to improve the image's contrast, 2) dividing the image into smaller parts using a sliding window and extracting features using a Stacked Sparse Autoencoder (SSAE), and 3) pooling the extracted features and using a classifier Support Vector Machine for classification. Our model results show that this method provides better performance in classifying the two populations. In the study, the model uses handcrafted potential features to diagnose osteoporosis such as Gabor filter features extracted considering different orientations from bone images. To obtain greater performance HOG and LPQ methods were also used. This technique used back-based optimization to carefully select features based on Fusion at the score and decision level of the model which achieved an overall accuracy of 89.66%

Delimayanti et al. [7] explained Previous research has shown that it is possible to predict or detect osteoporosis condition by evaluating the thickness of the clavicle cortex as observed in thorax X-ray images, but this approach is limited by its dependence on subjective visual assessments and the resolution of the X-ray images. So, to address these issues, this paper explores the use of algorithms based on image processing to classify Employing Gray Level Co-occurrence Matrix (GLCM) to analyse X-ray images, and K-Nearest Neighbour (KNN) as feature extraction techniques. The study has a small dataset of only 46 thorax images from 44 women and 2 male individuals, with an average age of 63 years, whose T-scores were previously measured using DEXA scans. The proposed method showed 100% sensitivity and 90% specificity in correctly classifying images using the measurement of clavicle cortex thickness with GLCM and KNN.

The overall accuracy in assessing osteoporosis was 97.83%, indicating a strong correlation with the predetermined T-scores from DEXA scans. The method uses image pressing techniques namely filtering, enhancing, Edge detecting, and rotation of images for data retrieval. Automatic measurement of the cartel thickness to classify the X-ray based on potential texture features is focused on in this methodology.

Ashames et al. [3] Diagnosing osteoporosis through X-ray images can be a difficult task because of the strong resemblance between the bone structures of healthy and osteoporotic patients. However, a successful diagnosis can be achieved by utilizing an effective data augmentation strategy along with deep transfer learning architecture. The study implemented rotations of 90 and 270 degrees in patches, as well as adjustments to contrast, brightness, and sharpness to increase the quantity of data used for training so can improvise the discriminatory information in the images. The results showed a significant improvement in accuracy as more data was used, with the highest accuracy of 99.02% being achieved using the ResNet50 model on a dataset of 1566 images. Furthermore, when a CNN model was trained from the beginning, it still showed good accuracy of 96.1%. These results demonstrate the best impact of this technique for artificially increasing the size of a dataset and show the potential for early diagnosis of osteoporosis using this methodology. The method uses a different data set that uses a region of Interest captured from the calcaneus bone region of X-ray images obtained from both normal and osteoporosis cases. Enhancement, and contrast adjustment where in world to uphold the X-ray images to capture the Unseen features important for classification. Different CNN architectures such as Inception V3, Alex Net, Google Net, Mobile Net, and Resnet50 were used in the study to evaluate the performance of the model.

Kumar et al. [18] The study aims to address the widespread problem of osteoporosis, a condition that causes the weakening of bone tissues, particularly among older individuals. Early detection of osteoporosis is crucial in reducing fractures and improving overall health outcomes. This study proposes a deep neural network approach to diagnose disease using X-rays, which are easily available and cost low for medical examinations. The methodology involves a deep learning model, Osteo-Net, which has skip connections and multiple blocks. This architecture leverages the strength of the model to extract important features from images, even if they are of low quality. The study's findings indicate that the model achieved a validation accuracy of 84.06% and a testing accuracy of 82.61% on test images, despite requiring less time for training. Moreover, the method was computationally efficient and cost-effective. It demonstrates promising results for screening osteoporosis and outperforms other existing methods. This deep neural network-based low-cost approach can serve as an alternative to the DXA tool, especially in healthcare centers that lack access to DXA machines. Osteoporosis is a disease that results in making the bone very sensitive by absorbing the Bone mass density and increasing the risk of fractures. Deep learning techniques help to analyze huge medical data and carefully bucket the normal and osteoporosis condition mostly the clinical data such as sex, age, lifestyle, and history are information captured along with X-ray images to predict the risk of fractures.

Liu et al. [21] Osteoporosis is a disease causing the weakening of bone tissues, has always been a topic of interest for researchers due to the important role that bone mineral density plays in its detection. However, the low contrast, noise in X-ray images, and the variation in bone shapes among patients can make it difficult for existing diagnosis

algorithms to produce reliable results. This study proposes an improved algorithm for osteoporosis diagnosis using the U-NET architecture.

The bones in X-rays are annotated to create the dataset. Input in each layer is normalized to maintain the stability of data distribution is maintained, allowing for accelerated training. The energy function is a mathematical expression evaluated using the Cross-entropy loss function, the SoftMax prediction class value is a useful tool for interpreting the output of a CNN and making predictions based on the high-level features extracted from the input data. Finally, the diagnostic result is obtained by extracting all segmented images. The improved U-NET was found to effectively address the issue with recognition rate for measuring bone mineral density, despite image interference, which was achieved at a certain level of 81% and better performance compared to other methods. The calculation of bone density is always on priority in research as it plays a key role in osteoporosis direct diagnosis. low-contrast makes the images noisier so it is difficult to get the expected results. So, the Author marked bone regions in the original images and the dataset is prepared. Later Normalization technique is used to ensure data is equally distributed in each layer lastly the energy is evaluated by using the SoftMax class for each separate class of feature map. Segmented results are evaluated to obtain a final osteoporosis diagnosis.

Yamamoto et al. [43] This method determines efficacy by using a deep neural network in diagnosing osteoporosis disease using hip X-ray and incorporating clinical data which enhances the performance compared to relying solely on the images. A dataset is taken from 1131 individuals that took hip radiography and BMD test values at the same hospital from the year 2014 to 2019. The diagnosis of osteoporosis was performed with 5 different convolutional neural networks (CNN) trained systems. Additionally, the impact of incorporating clinical data was evaluated by creating ensemble models combining each CNN with patient variables. Each model's Various evaluation metrics such as accuracy, precision, recall, specificity, negative predictive value (NPV), F1 score, and area under the curve (AUC) score were utilized to assess the performance of the five CNN models that used hip radiographs. The models were evaluated based on their ability to accurately identify patients with osteoporosis with high sensitivity and specificity. Google Net and Efficient Net b3 demonstrated the highest scores in these evaluation metrics in terms of accuracy, precision, and specificity. Efficient Net b3 was the top-performing ensemble model out of the five, achieving an accuracy of 88.5%. The findings indicate that convolutional neural network models can effectively diagnose osteoporosis considering hip X-rays inclusion of clinical data can enhance their performance even further. Certain limitations of the study are CNN model selection is being narrowed due to the availability of the clinical data also the selection of the model is challenging due to high contrast images which can be better evaluated with the presence of clinical data. There is overfitting in the model due to less availability of data. CNN model performs better with a large amount of data with better performance accuracy. So, increasing the number of images for further analysis is required. Pre-trained model Efficient Net b3 provided the best accuracy in comparison with other CNN models.

Jang et al. [15] This study aimed to determine if it is possible to diagnose osteoporosis through the use of simple hip X-rays using Deep learning. A dataset of 1001 female patients aged 55 years or older, each with both a DEXA scan and a matched hip radiograph, was collected. The images were divided into sets for training,

validation, and testing. A deep neural network model was developed using VGG16 and a nonlocal neural network. To evaluate the model's performance, accuracy, sensitivity, specificity, positive predictive value, and negative predictive value were all calculated, as well as a receiver operating characteristic curve. The final model had an accuracy of 81.2%, specificity of 68.9%, and sensitivity of 91.1%. The validation was done using 117 additional datasets confirming the model's performance with an accuracy of 71.8% the model also generated a value of 0.700. The results showed that the AUC score was high, and accurately predict the presence of osteoporosis in lab settings. Several limitations of the study are the values of BMD obtained from Dexa where from hip and spine but the only hip was considered for the study due to complexity in calculating the spine region BMD from the data. Also, the data taken from both regions will make the model difficult to evaluate. In this model without spine data, it works best as the screening tool since it is difficult to distinguish between osteopenia and osteoporosis the study is focused on osteoporosis, and the non-osteoporosis group as osteopenia classification is considered as a gray zone due to many similarities between osteopenia and osteoporosis also it requires large data in each group to make the model distinguish between minute similarities among the groups.

In this study, T-score is considered rather than BMD for classification. In this research paper, we utilized the effectiveness and affordability of X-ray imaging in conjunction with the power of CNN architectures to develop an early diagnosis tool for osteoporosis. Our study presented an annotated dataset using X-rays that are carefully categorized as normal and osteoporosis patients based on the T-score values taken from the DEXA machine. We experimented with five well-known CNN networks, namely VGG16, VGG19, DenseNet121, InceptionV3, and Resnet50, using Fastai, a PyTorch library, can be utilized to employ transfer learning and enable Convolutional Neural Networks (CNNs) to perform effectively despite having limited training data. We applied transfer learning to all Convolutional Neural Networks (CNNs) networks and compared the results to identify a suitable model for clinical osteoporosis detection. This study is the first to detect knee osteoporosis with a labelled dataset containing classes of osteoporosis. Section 2 elaborates Literature Review, while Section 3 discusses the dataset with different methods employed to analyse it. The experimental results are shown in Section 4, discussion with a comparison to the existing literature in Section 5. The paper concludes Finally, in Section 6.

3 Dataset preparation

The Data was collected from Zydus Hospital, Dahod, Gujarat. The dataset used in this study consisted of 830 simple radiographs, which were separated into two distinct groups based on T-score values obtained from DXA: the osteoporosis group, comprising subjects the participants were divided into two groups based on their T-scores: the osteoporosis group, which included individuals with a T-score of –2.5 or less, and the normal group, which included individuals with a T-score greater than –2.5 established by WHO. Out of the 830 subjects, 410 were osteoporosis, while the remaining 420 were considered normal. After obtaining X-rays from the hospital X-rays were classified based on the region such as the spine, hip, knee, hand, and leg joint. The resulting dataset comprised 830 knee X-rays, which were resized to the same dimensions.

Only X-rays were considered for the CNN-based classification model. The dataset was split into two separate sets: a training set and a validation set, and several CNNs, including VGG16, VGG19, DenseNet121, InceptionV3, and Resnet50, were trained on the separate training set to detect and classify Normal and Osteoporosis cases. The classifier's precision was assessed by validating it against the validation sets. Below in Figure 1 shows sample Dataset images of the Spine, Hand, Knee, Hip, and Leg for Normal and Osteoporosis cases.

3.1 Sample images

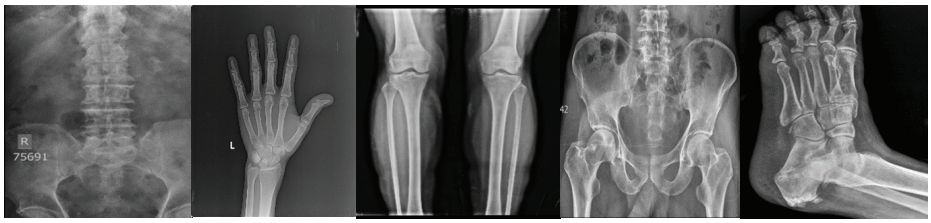

Fig. 1. Dataset images of normal and Osteoporosis cases

4 Proposed methodology

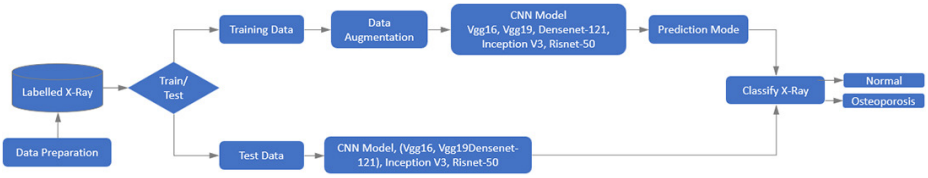

Fig. 2. Block diagram of CNN architecture

A model has been proposed to detect osteoporosis from X-rays illustrated in a block diagram in Figure 2.

Initially, a dataset of X-rays was collected and categorized into train and test sets. To enhance the train data, image augmentation was performed before feeding it to the CNN classifier. For a Deep learning model to be well-trained, it must possess high generalizability. Generalizability refers to the model's ability to accurately classify blind test data and the diversity of training data it has been exposed to improve the model's generalizability, it should be trained on a range of data variations, such as samples with different orientations or colour scales. If the training data does not include all possible versions of an image, the model may misclassify it. Overfitting is another issue with poorly generalizable models, where they may achieve high training accuracy but low validation accuracy. For a successful DL model, validation accuracy should increase with training accuracy, and the error obtained from validation error should decrease with training error. The technique of Data augmentation is helpful to improve a model's generalizability and prevent overfitting by exposing it to a different training data possibility. [14] The Convolutional Neural Network model is trained with the augmented train images. Finally, the metrics of the trained classifier were calculated

by analysing the prediction accuracy on the train and test images to determine the effectiveness of the model to classify normal and osteoporotic Cases. [30]

4.1 Transfer learning approach

Convolutional Neural Networks consist of three main layers that are convolutional, pooling, and fully connected. Convolution employs a group of filters to acquire features from input images. The pooling purpose is to reduce the spatial dimensionality of the output from the convolutional layer by enabling shift-invariance. Multiple convolution and pooling layers are stacked to extract higher-level feature maps. Fully connected layers are typically placed after the stacked convolutional and pooling layers in a CNN, and before the output, layer to carry out reasoning tasks. [37] In the domain of deep learning, transfer learning encompasses two primary types: Feature extraction and fine-tuning are both techniques commonly used in deep learning. [48] During the feature extraction standard dataset, ImageNet was used to remove the top classification layer. The remaining model is then treated as a feature extractor to invoke relevant features in the new dataset, and a new classification model is trained on the upper part of the pre-trained model for classifying purposes. Fine-tuning involves utilizing pre-trained model weights as primary values for training and later updating them as the process advances. During fine-tuning, the learned weights from the original dataset are used as a starting point, and then the weights are adjusted and fine-tuned to more precise features that are related to the new dataset. The objective is to adapt the general features to a specific one. [4] To avoid overfitting caused by limited training data, this study utilized pre-trained weights from ImageNet and applied a transfer learning strategy. For binary classification, the final layer of advanced models such as VGG16, VGG19, DenseNet121, InceptionV3, and ResNet50 was fine-tuned in this study by replacing the FC layers with SoftMax activation function and for regularization adding a dropout of 0.5. Finally, A layer with dense connections was added to implement the SoftMax activation function, producing two probability outputs for the "Normal" and "Osteoporosis" class. The forthcoming section will present an overview of the model's architecture and its use for binary classification.

Vgg16.

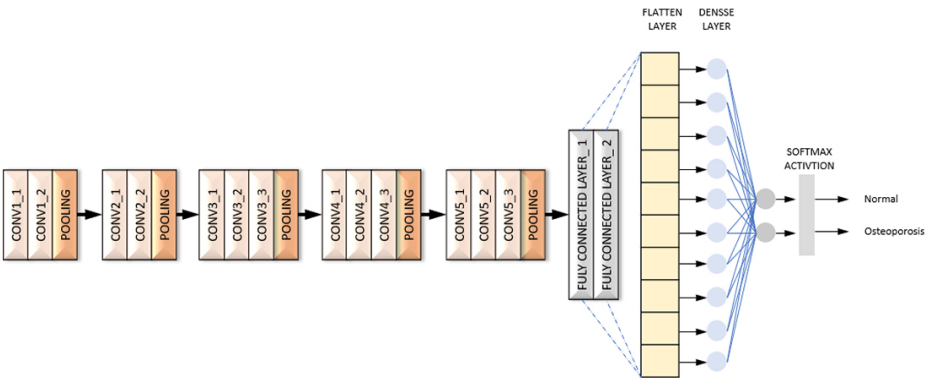

Fig. 3. VGG16 architecture for binary classification

The VggNet architecture is developed by the Visual Geometry Group proposed by Simonyan et al. [31]

The input to the network is an RGB image of 224 × 224 pixels. Convolution layers are arranged sequentially, with each layer having a small receptive field of 3 × 3 pixels and a stride of 1 pixel. The pooling layers, which perform downsampling, are interspersed between the convolutional layers. The FC layers are located at last to perform classification from learned features. The VGG16 architecture has 16 layers, which include 13 convolutional layers and 3 FC layers. [38] In addition to the convolutional layers, the model incorporates max-pooling layers to decrease the size of feature maps, and a SoftMax classifier is appended to the final layer, as shown in Figure 3.

Vgg19.

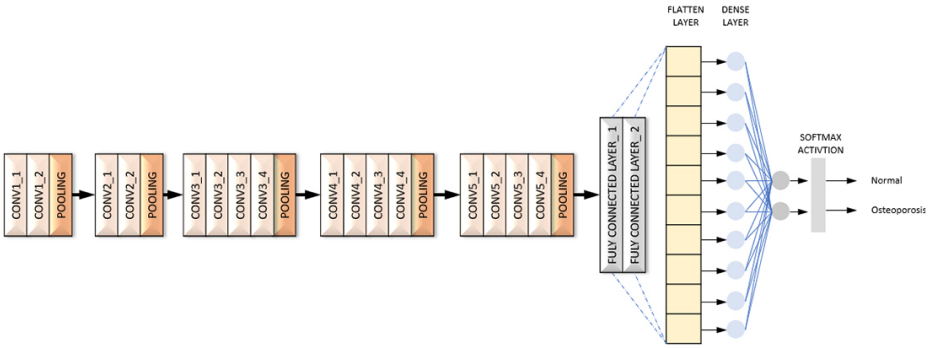

Fig. 4. VGG19 architecture for binary classification

VGG19 is an extension of the VGG16 architecture. It is widely used for image classification tasks. [31] The VGG19 architecture is similar to the VGG16 architecture but with more layers. The architecture of the model includes a sequence of convolutional layers and pooling layers, which are then succeeded by five fully connected layers. The input to the network is a fixed-size RGB image of 224 x 224 pixels. Convolution layers have a receptive field of 3 x 3 pixels and a stride of 1 pixel, and the pooling layers perform down sampling. The VGG19 architecture has a total of 19 layers, including 16 convolution layers and 3 FC layers. The model also includes a max-pooling layer to minimize the size of the feature maps, also a SoftMax classifier is appended to the final layer for classification. [29]

Overall, the VGG19 architecture is deeper than VGG16 and is capable of learning more complex features as shown in Figure 4.

DenseNet121.

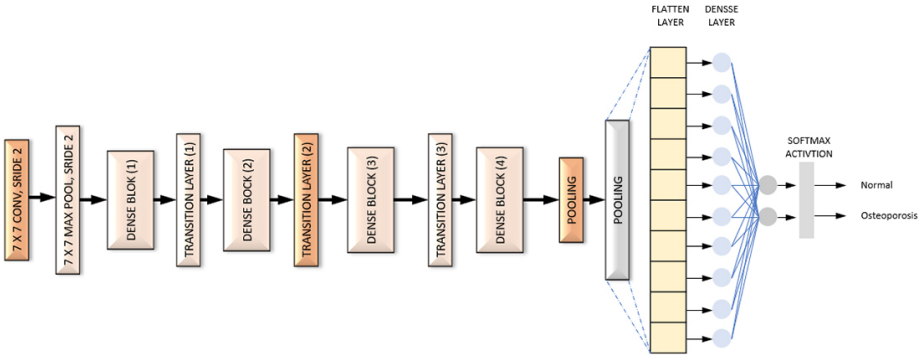

Fig. 5. DenseNet121 architecture for binary classification

DenseNet121. is a CNN architecture introduced in 2016 by Huang et al. It is a part of the Dense Net family of models that are designed to improve gradient flow and feature reuse in deep neural networks. The DenseNet121 architecture has many dense blocks, which are composed of densely connected convolutional layers. The input to the architecture is a fixed-size RGB image of 224 × 224 pixels. Each dense block includes multiple convolutional layers that are densely connected to all preceding layers, resulting in a high level of feature reuse and information flow. The transition layers, which are located between the dense blocks, use 1x1 convolutional layers to minimize the dimensionality of the feature maps and down sample the spatial resolution. The DenseNet121 architecture has 121 layers, 4 dense blocks, and 3 transition layers. The model also includes global average pooling, to average the feature maps across the spatial dimensions, and FC layer with SoftMax activation for classification. [26]

DenseNet121 is using fewer parameters than other deep learning models. In between the Dense Blocks are transition layers that use batch normalization for down-sampling as shown in Figure 5.

InceptionV3.

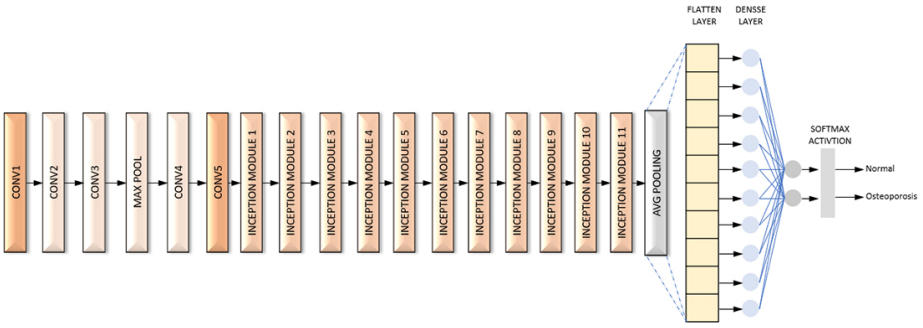

Fig. 6. InceptionV3 architecture for binary classification

InceptionV3 developed by researchers at Google including Christian Szegedy, InceptionV3 was developed by researchers at Google including Christian Szegedy,

Vincent Vanhoucke, Sergey Ioffe, Jonathon Shlens, and Zbigniew Wojna. It was first introduced in 2015 [33]. InceptionV3 is an image recognition deep neural network architecture composed of 11 inception modules, totalling 484 layers, and is designed to maintain network efficiency while reducing the number of parameters through factorized convolutions. [39] Additionally, InceptionV3 incorporates downsizing techniques to minimize the number of features. In the context of Normal and Osteoporosis classification, as depicted in Figure 6.

Resnet 50.

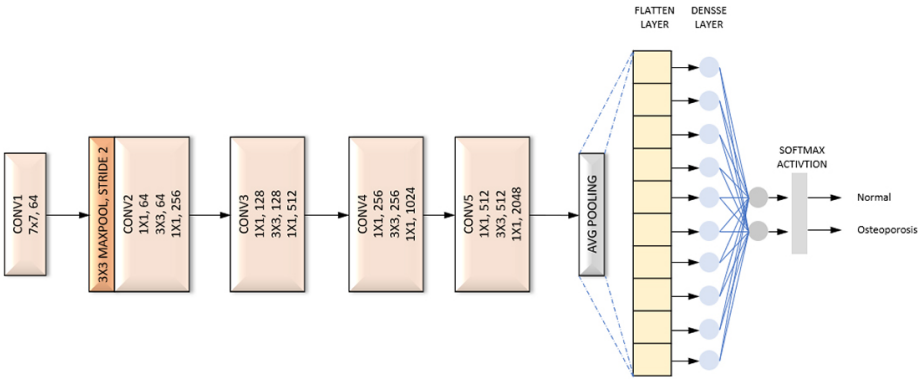

Fig. 7. ResNet50 architecture for binary classification

ResNet50 is a deep residual architecture for image classification, developed by Kaiming He, Xiangyu Zhang, Shaoqing Ren, and Jian Sun at Microsoft Research introduced in 2015 [11]. ResNet50 is an image classification deep residual neural network architecture, which is a variant of the Residual Network. It comprises 48 layers of convolution, along with a single MaxPool and single average pool layer. In this architecture, there are three convolutional layers in each convolution block and three convolutional layers in each identification block as well. [25] ResNet50 is a highly parameterized neural network, with over 23 million trainable parameters as illustrated in Figure 7.

Fastai is an open-source deep learning library that was proposed by Jeremy Howard and Rachel Thomas the library is constructed on PyTorch's core functionality and allows for simplified access to commonly used Deep learning methodologies, including image classification and natural language processing, are utilized and collaborative filtering. The advantage of Fastai is its ease of use, which allows individuals with limited programming experience to quickly and easily implement complex deep learning models. The library also provides several pre-trained models, as well as the ability to fine-tune these models for specific use cases [12].

5 Experiments and results

To assess the metrics of various CNN architectures to classify the Normal and Osteoporosis condition in X-rays, we conducted an experiment that involved four different architectures:

VggNet-16, VggNet-19, DenseNet121, Inception V2, and Resnet 50. Previous research has utilized these architectures to classify medical images for different diseases and thus are viable for diagnosis of osteoporosis in X-rays as well.

The Table 1 displays the error rates obtained by the models VggNet-16, VggNet-19, DenseNet121, Inception V2, and Resnet 50 for 10 epochs.

Table 1. The error rates obtained by the models VggNet-16, VggNet-19, DenseNet121, Inception V2, and Resnet 50 for 10 epochs

Model	Error Rate									
	Loss_1	Loss_2	Loss_3	Loss_4	Loss_5	Loss_6	Loss_7	Loss_8	Loss_9	Loss_10
VggNet-16	0.462344	0.53653	0.45397	0.51591	0.490201	0.453559	0.521193	0.34811	0.36317	0.203172
VggNet-19	0.123311	0.24362	0.40735	0.4483	0.317172	0.404575	0.347209	0.2279	0.17442	0.131246
DenseNet-121	0.435148	0.46261	0.41742	0.48815	0.463319	0.441293	0.387739	0.36914	0.24885	0.273061
ResNet-50	0.350949	0.41608	0.45701	0.38245	0.431703	0.377549	0.344276	0.21192	0.29203	0.280373
Inception V3	0.292946	0.20481	0.31905	0.31845	0.329495	0.258551	0.325711	0.31633	0.15178	0.121697

The Table 2 displays the validation loss obtained by the models VggNet-16, VggNet-19, DenseNet121, Inception V2, and Resnet 50 for 10 epochs.

Table 2. The validation loss obtained by the models VggNet-16, VggNet-19, DenseNet121, Inception V2, and Resnet 50 for 10 epochs

Model	Validation Loss									
	error-1	error-2	error-3	error-4	error-5	error-6	error-7	error-8	error-9	error-10
VggNet-16	2.628969	3.68144	0.70757	0.89141	0.806532	0.660667	2.664589	0.71722	1.74969	1.709694
VggNet-19	1.909579	1.26244	1.77654	1.25762	0.618869	0.590911	1.539555	0.62052	0.7515	0.74368
DenseNet-121	1.720623	0.70765	2.77013	0.69067	1.711715	0.655901	1.606874	0.5008	0.55696	0.673484
ResNet-50	1.720623	0.70765	2.77013	0.69067	0.711715	0.655901	2.606874	0.5008	0.55696	0.673484
Inception V3	1.658528	0.58528	2.56516	1.58447	0.546249	0.508088	0.573194	0.59018	1.4886	0.422821

The Table 3 displays the accuracy obtained by the models VggNet-16, VggNet-19, DenseNet121, Inception V2, and Resnet 50 for 10 epochs.

Table 3. The accuracy obtained by the models VggNet-16, VggNet-19, DenseNet121, Inception V2, and Resnet 50 for 10 epochs

Model	Accuracy									
	Epoch-1	Epoch – 2	Epoch-3	Epoch – 4	Epoch – 5	Epoch – 6	Epoch – 7	Epoch – 8	Epoch – 9	Epoch – 10
VggNet-16	69%	66%	69%	66%	**72%**	65%	68%	71%	72%	71%
VggNet-19	65%	55%	71%	69%	71%	65%	74%	**77%**	77%	74%
DenseNet-121	72%	69%	71%	72%	74%	71%	74%	78%	**83%**	73%
ResNet-50	52%	65%	68%	77%	71%	72%	77%	**82%**	75%	77%
Inception V3	71%	69%	72%	77%	74%	**88%**	74%	77%	85%	81%

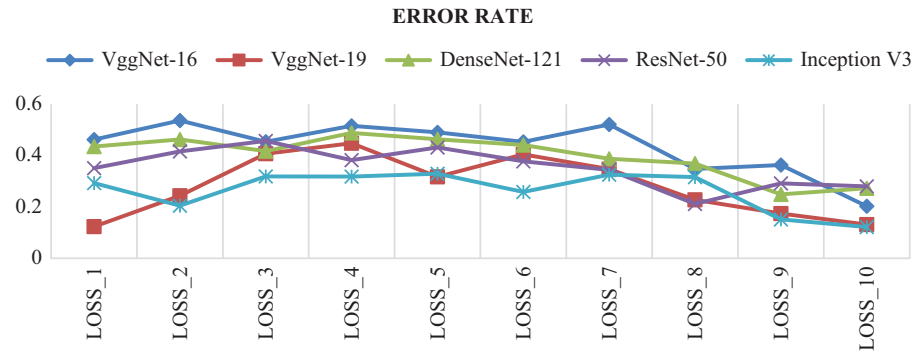

Fig. 8. The graph displays the error rates obtained by the models VggNet-16, VggNet-19, DenseNet121, Inception V2, and Resnet 50 for 10 epochs

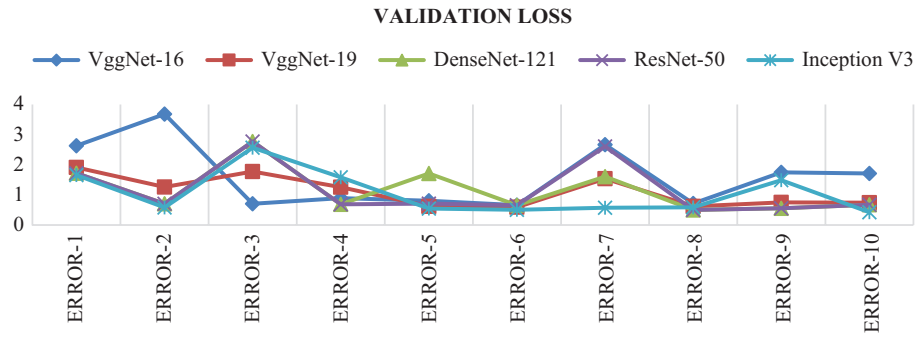

Fig. 9. The graph displays the Validation Loss obtained by the models VggNet-16, VggNet-19, DenseNet121, Inception V2, and Resnet 50 for 10 epochs

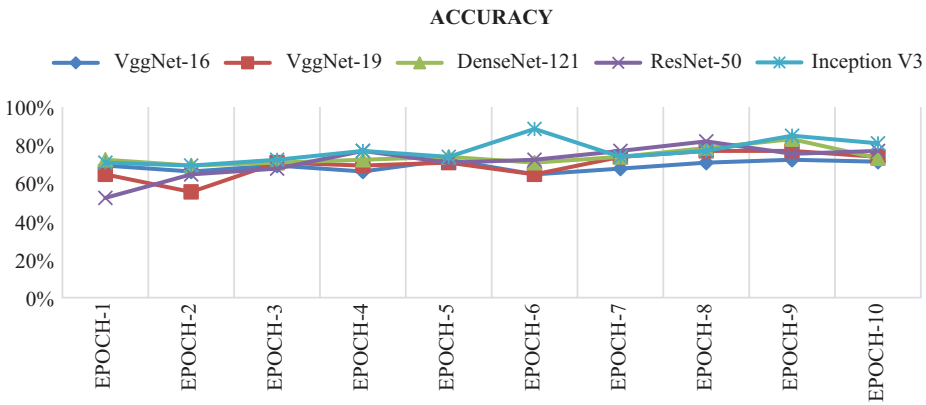

Fig. 10. The graph displays the accuracy obtained by the models VggNet-16, VggNet-19, DenseNet121, Inception V2, and Resnet 50 for 10 epochs

Table 4 displays the error rates obtained by the models VggNet-16, VggNet-19, DenseNet121, Inception V2, and Resnet 50 for 10 epochs.

Table 4. The error rates obtained by the models VggNet-16, VggNet-19, DenseNet121, Inception V2, and Resnet 50 for 10 epochs

Model	Error Rate									
	Loss_1	Loss_2	Loss_3	Loss_4	Loss_5	Loss_6	Loss_7	Loss_8	Loss_9	Loss_10
VggNet-16	0.49295	0.40461	0.41905	0.41845	0.389446	0.2168	0.42571	0.395625	0.35178	0.20648
VggNet-19	0.35029	0.39226	0.25579	0.35348	0.416144	0.38498	0.38368	0.249421	0.21532	0.1133
DenseNet-121	0.48439	0.46792	0.35028	0.33316	0.272229	0.26748	0.23474	0.078248	0.03988	0.10122
ResNet-50	0.40246	0.36237	0.37255	0.48549	0.475715	0.39344	0.27247	0.213338	0.12098	0.20394
Inception V3	0.44547	0.43832	0.46148	0.34275	0.210794	0.37141	0.24565	0.130906	0.11031	0.96845

Table 5 displays the validation loss obtained by the models VggNet-16, VggNet-19, DenseNet121, Inception V2, and Resnet 50 for 10 epochs.

Table 5. The validation loss obtained by the models VggNet-16, VggNet-19, DenseNet121, Inception V2, and Resnet 50 for 10 epochs

Model	Validation Loss									
	error-1	error-2	error-3	error-4	error-5	error-6	error-7	error-8	error-9	error-10
VggNet-16	3.65853	2.58528	2.56516	2.58447	1.546249	0.55809	1.57319	1.590177	0.5886	0.69282
VggNet-19	2.49631	2.58953	3.67135	1.63781	2.668154	1.62149	0.6101	0.687407	1.59679	0.59679
DenseNet-121	1.52666	1.62154	1.61183	2.52561	1.548791	2.56726	0.56702	0.570521	0.42947	0.41522
ResNet-50	1.28868	0.98218	1.0122	1.91268	0.68418	0.61781	0.58332	0.539041	0.50485	0.52596
Inception V3	1.00201	0.79292	0.72642	0.74127	0.786581	0.63614	1.51236	0.493816	1.49798	0.60845

All deep learning models, including VGG16, VGG19, DenseNet121, Inception-ResNet-V2, InceptionV3, ResNet50, and Xception, were trained using a 12 GB NVIDIA Tesla K80 GPU in the study. The training was performed on all images, and this GPU was able to handle the computations required for the training process with all images in the dataset resized to 224 × 224 pixels. The CNN learner function from the Fastai library was used to load the CNN architectures, and data augmentation was employed using the Data loader ().

Table 6 displays the Accuracy obtained by the models VggNet-16, VggNet-19, Dense net 121, Inception V2, and Resnet 50 for 10 epochs.

Table 6. The Accuracy obtained by the models VggNet-16, VggNet-19, DenseNet121, Inception V2, and Resnet 50 for 10 epochs

Model	Accuracy									
	Epoch-1	Epoch – 2	Epoch-3	Epoch – 4	Epoch – 5	Epoch – 6	Epoch – 7	Epoch – 8	Epoch – 9	Epoch – 10
VggNet-16	71%	69%	72%	77%	74%	**78%**	74%	77%	77%	77%
VggNet-19	74%	77%	82%	77%	75%	75%	77%	84%	82%	**86%**
DenseNet-121	73%	78%	79%	72%	82%	72%	83%	**93%**	77%	88%
ResNet-50	62%	63%	73%	66%	71%	75%	77%	82%	**89%**	78%
Inception V3	68%	71%	69%	65%	72%	75%	75%	78%	83%	**90%**

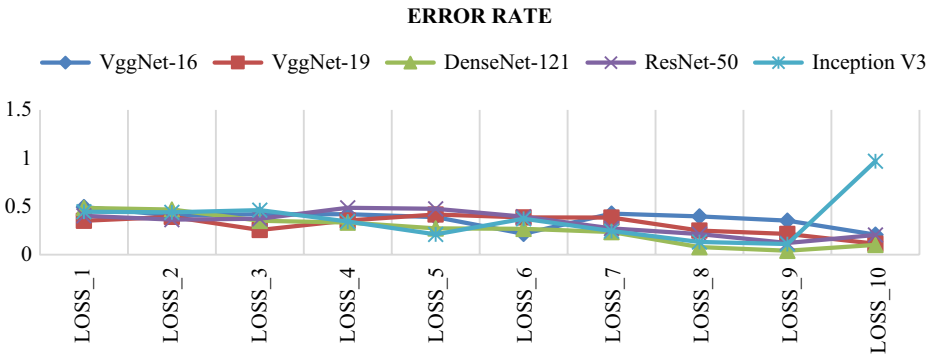

Fig. 11. The graph displays the error rate obtained by the models VggNet-16, VggNet-19, DenseNet121, Inception V2, and Resnet 50 for 10 epochs

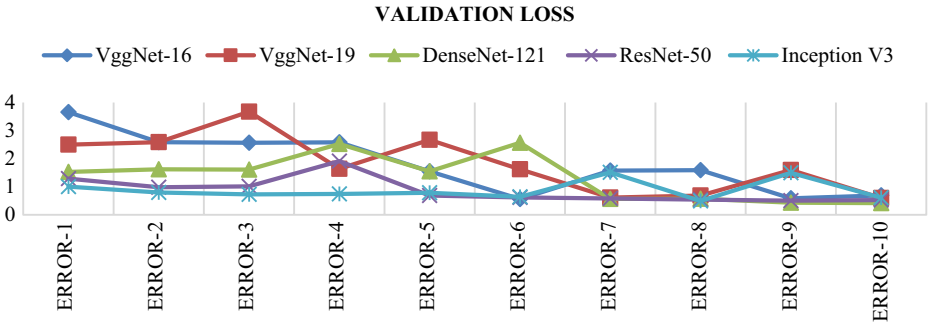

Fig. 12. The graph displays the Validation Loss obtained by the models VggNet-16, VggNet-19, DenseNet121, Inception V2, and Resnet 50 for 10 epochs

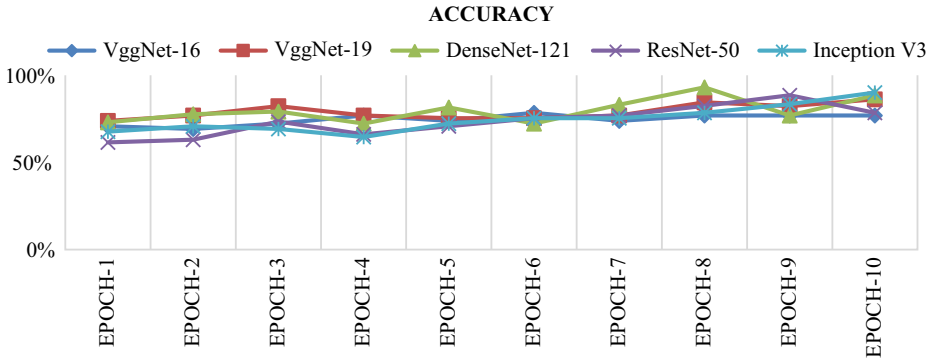

Fig. 13. The graph displays the Accuracy obtained by the models VggNet-16, VggNet-19, DenseNet121, Inception V2, and Resnet 50 for 10 epochs

The dataset is split into a 90:10 ratio of train and validation sets due to the small sample size. [42] The CNN architectures, including VggNet-16, VggNet-19, DenseNet121, Inception V2, and Resnet 50, were first trained only on the train set of images for 10 epochs. Accuracy, error rate, and validation loss were the performance metrics used to evaluate the CNNs, which were trained with pre-trained networks from the ImageNet dataset to evaluate the effect of transfer learning on classification performance, the results were displayed in tables [4, 5, 6] form and graphically in figures [11, 12, 13]. The tables and figures show the results of the Model not initially pre-trained with the ImageNet dataset, while the results concerning the pre-trained Model are also shown in tables [1, 2, 3] and displayed graphically in figures. [8, 9, 10].

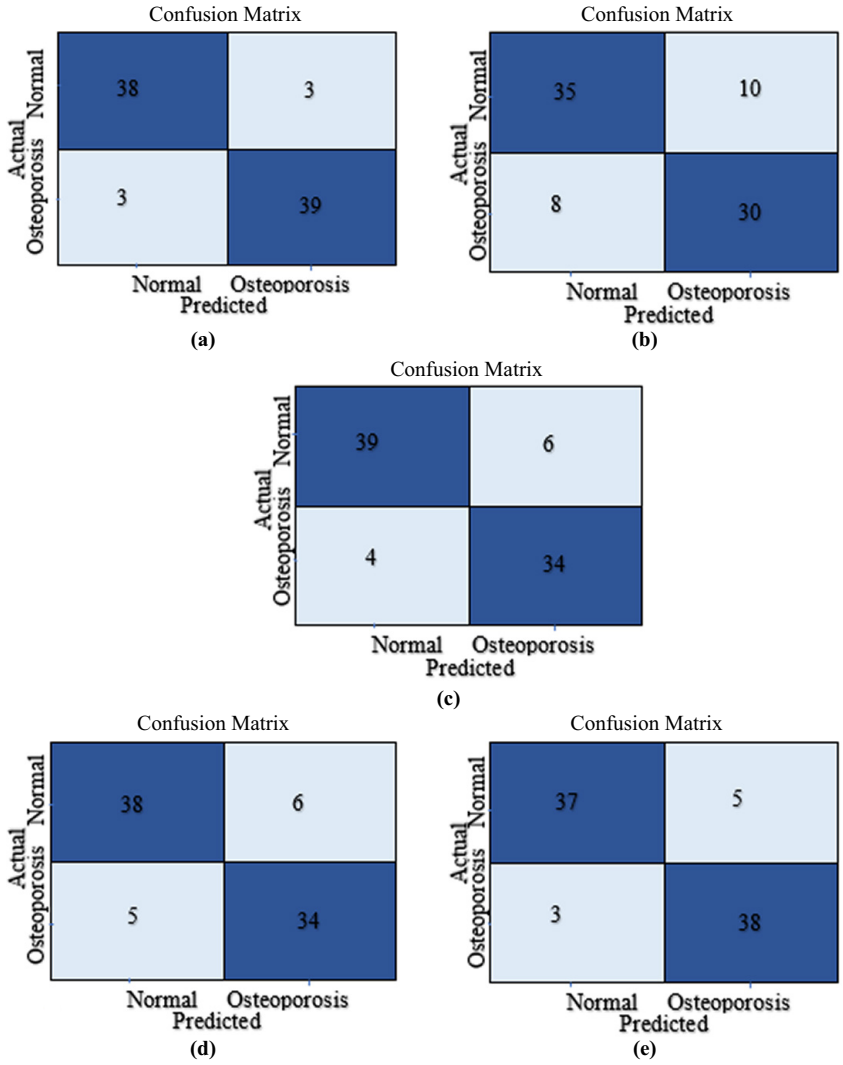

Fig. 14. The validation set of the dataset was used to generate confusion matrices a. DenseNet121, b. Inception V3, c. ResNet50, d. Vgg-16 e. Vgg-19

The confusion matrix for VggNet-16, VggNet-19, DenseNet121, Inception V2, and Resnet 50 models calculated using validation sets in pre-trained CNNs is displayed in Figure 14. It can be observed by the confusion matrix that normal disease group and osteoporosis disease group images were better classified by the CNN architectures. [28] The results suggest that X-ray images are effective in identifying osteoporosis based on the performance of all the CNN architectures as shown in Table 7.

5.1 Discussion

Our dataset contains both image and numerical data and other important factors. However, our model focused on creating a deep learning-based model to diagnose osteoporosis from X-ray images. Our system uses a Binary classification system based on T-score values from the DEXA system. The X-rays used in our study come from both genders and various age groups, from 18 to 92 years old. [8]

Table 7. A comparison was made between the metrics of regular CNN and pre-trained CNN

	Normal CNN			**Pre-trained CNN**		
Model	**Accuracy**	**Error rate**	**Validation Loss**	**Accuracy**	**Error rate**	**Validation Loss**
VggNet-16	72%	0.4902	0.80653	78%	0.216801	0.558088
VggNet-19	77%	0.2279	0.62052	86%	0.13296	0.596791
DenseNet-121	83%	0.24885	0.55696	93%	0.078248	0.41522
ResNet-50	82%	0.21192	0.5008	89%	0.120976	0.504849
Inception V3	88%	0.25855	0.50809	90%	0.96845	0.60845

Based on Figures 8 and 11, we visualize that DenseNet121, achieved the best classification results, while VGG-19 and VGG-16 showed the lowest performance in normal and pre-trained CNNs. Table 7 summarizes the performance Evaluations. The results show that DenseNet121, Resnet 50, Inception V3, and VGGNet-19 achieved the best classification accuracies of 83%, 82%, 88%, 77%, and 93%, 89%, 90%, and 86% for normal CNN and pre-trained CNN. The model's lowest error rates were 0.24885, 0.21192, 0.25855, 0.2279, and 0.078248, 0.120976, 0.96845, and 0.13296 for normal CNN and pre-trained CNN. The lowest validation loss was observed for DenseNet121, ResNet 50, Inception V3, and VGG-19, which were 0.55696, 0.5008, 0.50809, 0.62052, and 0.41522, 0.504849, 0.60845, 0.596791 for normal and pre-trained CNN. The results suggest that utilizing pre-trained CNNs and training them with the X-ray dataset led to higher accuracy as compared to training the CNNs from the beginning.

By achieving a classification accuracy of 93%, DenseNet121, demonstrates the viability of using CNNs for X-ray image classification.

Table 8. Presents our work comparison with existing state-of-the-art works in this area

Author	Year	Bone Type	Image Type	Classifier	Performance
C.tang et al	2020	lumbar vertebra	CT Images	BMDC-Net C.	76.65%
T Vishnu et al	2015	Hip,toe,elbow	X-ray Images	ANN classifier-based CAD system	90%
Keni Zheng et al	2016	Patches	X-ray Images	CFS-BF	79.30%
Peng Chu et al	2018	Dental Panoramic Radiographs	DPR image	Octuplet Siamese Network	89.80%
Ran Su et al	2020	Patches	X-ray Images	Alexnet	77.5%,
Naofumi Tomita et al	2018	chest, abdomen, and pelvis	CT Images	OVF detection system	89.20%
Frighetto-Pereira et al	2016	lumbar vertebral	MRI Images	RBF network	82.70%
Chelsea E et al	2022	Patches	X-ray Images	InceptionV3-SLESA	72.67%.
Linyan Xue et al	2022	vertebral bodies	CT Images	DSNet	83.40%
Pretrained CNN1	2023	**Spine,Knee,Hand,leg,Hip**	**X-ray**	VggNet-16	78%
Pretrained CNN2	2023	**Spine,Knee,Hand,leg,Hip**	**X-ray**	VggNet-19	86%
Pretrained CNN3	2023	**Spine,Knee,Hand,leg,Hip**	**X-ray**	DenseNet-121	93%
Pretrained CNN4	2023	**Spine,Knee,Hand,leg,Hip**	**X-ray**	ResNet-50	89%
Pretrained CNN5	2023	**Spine,Knee,Hand,leg,Hip**	**X-ray**	Inception V3	90%

6 Conclusion

Our research aimed to evaluate and compare the diagnosis of popular CNN models such as VggNet-16, VggNet-19, DenseNet121, Inception V2, and Resnet 50 models for detecting osteoporosis using X-rays. The images in our study were obtained from a custom dataset, which was categorized as normal, and osteoporosis groups based on the T-score calculated using the Dexa, a WHO-recognized BMD test for Osteoporosis Diagnosis. The dataset included a total of 830 X-ray images, results referred that DenseNet121 achieved the highest accuracy of 91%, while VggNet-19 had the lowest accuracy of 93.4%. Overall, the results indicate that Transfer learning with CNNs for diagnosing osteoporosis from X-ray can be an accessible and cost-effective diagnostic tool. Moving forward, there is potential for collecting more data, particularly from normal and osteoporotic subjects, to improve the diagnostic accuracy of the CNN models. Furthermore, a system could be developed that combines clinical factors with images to enhance the accuracy of osteoporosis detection.

7 Acknowledgements

The authors are thankful to Dr. Shivanand Dodamani and Dr. Vivek Patil to provide us valuable feedback and supporting in obtaining Ethical clearance certificate and Data from Zydus Hospital, Dahod, and Vivek Diagnostic Centre, Hubli. India.

8 References

[1] Adams, J. E. (2013). Advances in bone imaging for osteoporosis. Nature Reviews Endocrinology, 9(1), 28–42. https://doi.org/10.1038/nrendo.2012.223

[2] Albashish, D., Al-Sayyed, R., Abdullah, A., Ryalat, M. H., & Almansour, N. A. (2021). Deep CNN model based on VGG16 for breast cancer classification. In 2021 International Conference on information technology (ICIT) (pp. 805–810). IEEE. https://doi.org/10.1109/ICIT52682.2021.9491631

[3] Ashames, M. M., Ceylan, M., & Jennane, R. (2021). Deep transfer learning and majority voting approach for osteoporosis classification. International Journal of Intelligent Systems and Applications in Engineering, 9(4), 1–11. https://doi.org/10.18201/ijisae.2021473646

[4] Bengio, Y. (2012). Deep learning of representations for unsupervised and transfer learning. In Proceedings of ICML workshop on unsupervised and transfer learning (pp. 17–36). JMLR Workshop and Conference Proceedings. http://jmlr.org/proceedings/papers/v27/bengio12a/bengio12a.pdf

[5] Blake, G. M., & Fogelman, I. (2007). The role of DXA bone density scans in the diagnosis and treatment of osteoporosis. Postgraduate Medical Journal, 83(982), 509–517. https://doi.org/10.1136/pgmj.2007.057505

[6] Chu, P., Bo, C., Liang, X., Yang, J., Megalooikonomou, V., Yang, F., … & Ling, H. (2018). Using octuplet siamese network for osteoporosis analysis on dental panoramic radiographs. In 2018 40th Annual International Conference of the IEEE Engineering in Medicine and Biology Society (EMBC) (pp. 2579–2582). IEEE. https://doi.org/10.1109/EMBC.2018.8512856

[7] Delimayanti, M. K. (2017). Feature extraction and classification of thorax x-ray image in the assessment of osteoporosis. In 2017 4th International Conference on electrical engineering, computer science, and Informatics (EECSI) (pp. 1–5). IEEE. https://doi.org/10.1109/EECSI.2017.8239157

[8] Ferrari, S., Libanati, C., Lin, C. J. F., Brown, J. P., Cosman, F., Czerwiński, E., … & Lewiecki, E. M. (2019). Relationship between bone mineral density T-score and nonvertebral fracture risk over 10 years of denosumab treatment. Journal of Bone and Mineral Research, 34(6), 1033–1040. https://doi.org/10.1002/jbmr.3713

[9] Frighetto-Pereira, L., Rangayyan, R. M., Metzner, G. A., de Azevedo-Marques, P. M., & Nogueira-Barbosa, M. H. (2016). Shape, texture, and statistical features for classification of benign and malignant vertebral compression fractures in magnetic resonance images. Computers in Biology and Medicine, 73. https://doi.org/10.1016/j.compbiomed.2016.04.006

[10] Harris, C. E., & Makrogiannis, S. (2022, June). Sparse analysis of block-boosted deep features for osteoporosis classification. In 2022 IEEE 14th Image, Video, and Multidimensional Signal Processing Workshop (IVMSP) (pp. 1–5). IEEE. https://doi.org/10.1109/IVMSP54334.2022.9816199

[11] He, K., Zhang, X., Ren, S., & Sun, J. (2016). Deep residual learning for image recognition. In Proceedings of the IEEE conference on computer vision and pattern recognition (pp. 770–778). https://doi.org/10.1109/CVPR.2016.90

[12] Howard, J., & Gugger, S. (2020). Deep Learning for Coders with Fastai and PyTorch. O'Reilly Media.

[13] Huang, G., Liu, Z., Van Der Maaten, L., & Weinberger, K. Q. (2017). Densely connected convolutional networks. In Proceedings of the IEEE conference on computer vision and pattern recognition (pp. 4700–4708). https://doi.org/10.1109/CVPR.2017.243

[14] Inoue, H. (2018). Data augmentation by pairing samples for image classification. arXiv preprint arXiv:1801.02929.

[15] Jang, R., Choi, J. H., Kim, N., Chang, J. S., Yoon, P. W., & Kim, C. H. (2021). Prediction of osteoporosis from simple hip radiography using a deep learning algorithm. Scientific reports, 11(1), 19997. https://doi.org/10.1038/s41598-021-99549-6

[16] Kramer, R. S. S., Wagemans, J., & van der Helm, P. A. (2010). The effects of presentation time on memory for faces and objects: A meta-analysis. Cognitive, Affective, & Behavioral Neuroscience, 10(4), 441–458. https://doi.org/10.3758/CABN.10.4.441

[17] Dodamani, P. S., & Danti, A. (2022). Diagnosis of Osteoporosis from X-ray Images using Automated Techniques. In 2022 International Conference on Machine Learning, Big Data, Cloud and Parallel Computing (COM-IT-CON) (Vol. 1, pp. 1–5). IEEE. https://doi.org/10.1109/COM-IT-CON54601.2022.9850579

[18] Kumar, A., Joshi, R. C., Dutta, M. K., Burget, R., & Myska, V. (2022, July). Osteo-Net: A Robust Deep Learning-Based Diagnosis of Osteoporosis Using X-ray Images. In 2022 45th International Conference on Telecommunications and Signal Processing (TSP) (pp. 91–95). IEEE. https://doi.org/10.1109/TSP55681.2022.9851342

[19] Lee, S., Choe, E. K., Kang, H. Y., Yoon, J. W., & Kim, H. S. (2020). The exploration of feature extraction and machine learning for predicting bone density from simple spine X-ray images in a Korean population. Skeletal Radiology, 49, 613–618. https://doi.org/10.1007/s00256-019-03342-6

[20] Liu, J., Wang, J., Ruan, W., Lin, C., & Chen, D. (2020). Diagnostic and gradation model of osteoporosis based on improved deep U-Net network. Journal of Medical Systems, 44, 1–7. https://doi.org/10.1007/s10916-019-1502-3

[21] Mascarenhas, S., & Agarwal, M. (2021, November). A comparison between VGG16, VGG19, and ResNet50 architecture frameworks for Image Classification. In 2021 International Conference on Disruptive Technologies for Multi-Disciplinary Research and Applications (CENTCON) (Vol. 1, pp. 96–99). IEEE. https://doi.org/10.1109/CENTCON52345.2021.9687944

[22] Mebarkia, M., Meraoumia, A., Houam, L., & Khemaissia, S. (2023). X-ray image analysis for osteoporosis diagnosis: From shallow to deep analysis. Displays, 76, 102343. https://doi.org/10.1016/j.displa.2022.102343

[23] Rachner, T. D., Khosla, S., & Hofbauer, L. C. (2011). Osteoporosis: Now and the future. The Lancet, 377(9773), 1276–1287. https://doi.org/10.1016/S0140-6736(10)62349-5

[24] Reddy, A. S. B., & Juliet, D. S. (2019, April). Transfer learning with ResNet-50 for malaria cell-image classification. In 2019 International Conference on Communication and Signal Processing (ICCSP) (pp. 0945–0949). IEEE. https://doi.org/10.1109/ICCSP.2019.8698074

[25] Rochmawanti, O., & Utaminingrum, F. (2021, September). Chest X-Ray Image to Classify Lung Diseases in Different Resolution Sizes using DenseNet-121 Architectures. In 6th International Conference on Sustainable Information Engineering and Technology 2021 (pp. 327–331). https://doi.org/10.1145/3479645.3479667

[26] Dodamani, P. S., & Danti, A. (2021). Assessment of Bone Mineral Density in X-ray Images using Image Processing. In 2021 8th International Conference on Computing for Sustainable Global Development (INDIACom). IEEE.

[27] Salmon, B. P., Kleynhans, W., Schwegmann, C. P., & Olivier, J. C. (2015, July). Proper comparison among methods using a confusion matrix. In 2015 IEEE International Geoscience and Remote Sensing Symposium (IGARSS) (pp. 3057–3060). IEEE. https://doi.org/10.1109/IGARSS.2015.7326623

[28] Shaha, M., & Pawar, M. (2018, March). Transfer learning for image classification. In 2018 Second International Conference on Electronics, Communication and Aerospace Technology (ICECA) (pp. 656–660). IEEE. https://doi.org/10.1109/ICECA.2018.8474802

[29] Sharma, N., Jain, V., & Mishra, A. (2018). An analysis of convolutional neural networks for image classification. Procedia Computer Science, 132, 377–384. https://doi.org/10.1016/j.procs.2018.05.192

[30] Simonyan, K., & Zisserman, A. (2014). Very deep convolutional networks for large-scale image recognition. arXiv preprint arXiv:1409.1556.

[31] Su, R., Liu, T., Sun, C., Jin, Q., Jennane, R., & Wei, L. (2020). Fusing convolutional neural network features with hand-crafted features for osteoporosis diagnoses. Neurocomputing, 385, 300–309. https://doi.org/10.1016/j.neucom.2019.11.053

[32] Szegedy, C., Ioffe, S., Vanhoucke, V., & Alemi, A. (2017, February). Inception-v4, inception-resnet, and the impact of residual connections on learning. In Proceedings of the AAAI conference on artificial intelligence (Vol. 31, No. 1). https://doi.org/10.1609/aaai.v31i1.11231

[33] Talo, M. (2019). Automated classification of histopathology images using transfer learning. Artificial Intelligence in Medicine, 101, 101743. https://doi.org/10.1016/j.artmed.2019.101743

[34] Tang, C., Zhang, W., Li, H., Li, L., Li, Z., Cai, A., … & Yan, B. (2021). CNN-based qualitative detection of bone mineral density via diagnostic CT slices for osteoporosis screening. Osteoporosis International, 32, 971–979. https://doi.org/10.1007/s00198-020-05673-w

[35] Tomita, N., Cheung, Y. Y., & Hassanpour, S. (2018). Deep neural networks for automatic detection of osteoporotic vertebral fractures on CT scans. Computers in Biology and Medicine, 98, 8–15. https://doi.org/10.1016/j.compbiomed.2018.03.007

[36] Torrey, L., & Shavlik, J. (2010). Transfer learning. In Handbook of research on machine learning applications and trends: Algorithms, methods, and techniques (pp. 242–264). IGI Global. https://doi.org/10.4018/978-1-60566-766-9.ch012

[37] Vishnu, T., Saranya, K., Arunkumar, R., & Devi, M. G. (2015, November). Efficient and early detection of osteoporosis using trabecular region. In 2015 Online International Conference on Green Engineering and Technologies (IC-GET) (pp. 1–5). IEEE. https://doi.org/10.1109/GET.2015.7453840

[38] Wang, C., Chen, D., Hao, L., Liu, X., Zeng, Y., Chen, J., & Zhang, G. (2019). Pulmonary image classification based on inception-v3 transfer learning model. IEEE Access, 7, 146533–146541. https://doi.org/10.1109/ACCESS.2019.2942322

[39] Wani, I. M., & Arora, S. (2022). Osteoporosis diagnosis in knee X-rays by transfer learning based on convolution neural network. Multimedia Tools and Applications, 1–25. https://doi.org/10.1007/s11042-022-12953-6

[40] Xue, L. Y., Hou, Y., Wang, S. W., Luo, C., Xia, Z. Y., Qin, G., … & Yang, K. (2022). A dual-selective channel attention network for osteoporosis prediction in computed tomography images of the lumbar spine. Acadlore Trans. Mach. Learn, 1(1), 30–39. https://doi.org/10.56578/ataiml010105

[41] Yuan, C., Wu, Y., Qin, X., Qiao, S., Pan, Y., Huang, P., … & Han, N. (2019). An effective image classification method for shallow densely connected convolution networks through squeezing and splitting techniques. Applied Intelligence, 49, 3570–3586. https://doi.org/10.1007/s10489-019-01468-7

[42] Yamamoto, N., Sukegawa, S., Kitamura, A., Goto, R., Noda, T., Nakano, K., … & Ozaki, T. (2020). Deep learning for osteoporosis classification using hip radiographs and patient clinical covariates. Biomolecules, 10(11), 1534. https://doi.org/10.3390/biom10111534

[43] Zhang, B., Yu, K., Ning, Z., Wang, K., Dong, Y., Liu, X., … & Zhang, S. (2020). Deep learning of lumbar spine X-ray for osteopenia and osteoporosis screening: A multicenter retrospective cohort study. Bone, 140, 115561. https://doi.org/10.1016/j.bone.2020.115561

[44] Zheng, K., & Makrogiannis, S. (2016, August). Bone texture characterization for osteoporosis diagnosis using digital radiography. In 2016 38th Annual International Conference of the IEEE Engineering in Medicine and Biology Society (EMBC) (pp. 1034–1037). IEEE. https://doi.org/10.1109/EMBC.2016.7590927

[45] Auf der Strasse, W., Campos, D. P., Mendonça, C. J. A., Mendes, J., Soni, J. F., & Nohama, P. (2020). Thermal variations in osteoporosis after Aclasta® administration: Case study. International Journal of Online Biomedical Engineering and Technology, 16(10), 82–95. https://doi.org/10.3991/ijoe.v16i10.14635

[46] Kumarasinghe, K. A. S. H., Kolonne, S. L., Fernando, K. C. M., & Meedeniya, D. (2022). U-Net based chest X-ray segmentation with ensemble classification for Covid-19 and Pneumonia. International Journal of Online and Biomedical Engineering, 18(7). https://doi.org/10.3991/ijoe.v18i07.30807

[47] Wong, L., Ccopa, A., Diaz, E., Valcarcel, S., Mauricio, D., & Villoslada, V. (2023). Deep learning and transfer learning methods to effectively diagnose cervical cancer from liquid-based cytology pap smear images. International Journal of Online and Biomedical Engineering, 19(4). https://doi.org/10.3991/ijoe.v19i04.37437

9 Authors

Pooja S Dodamani, currently pursuing Ph.D. from Christ University Bangalore in the Department of Computer Science and Engineering. Medical Image Processing is the main area of research (Email: pooja.dodamani@res.christuniversity.in).

Dr. Ajit Danti is a Professor in the Department of Computer Science and Engineering, at Christ University Bangalore. 30 years of experience in Academics, Research & Administration at reputed Engineering colleges in India and abroad. Research interest includes Artificial intelligence, Machine learning, Computer Vision, etc. (email: ajitdanti@christuniversity.in).

Article submitted 2023-02-28. Resubmitted 2023-04-18. Final acceptance 2023-04-18. Final version published as submitted by the authors.